System Performance Modeling of the Lunar Flashlight CubeSat Instrument

Quentin Vinckier (Jet Propulsion Laboratory, California Institute of Technology – vinckier@jpl.nasa.gov)

Paul O. Hayne (University of Colorado), Jose M. Martinez-Camacho, Christopher Paine, R. Glenn Sellar, Udo J. Wehmeier (Jet Propulsion Laboratory, California Institute of Technology), Barbara A. Cohen (NASA Goddard Space Flight Center)

Lunar Flashlight (LF) mission

- **Goal ?** Detect, quantify and map surface H_2O ice in the PSRs (Permanently-Shadowed Regions) – where previous missions have already revealed strong indications of H_2O ice presence [1-6] – and occasionally sunlit regions of the lunar South Pole.
- **How ?** By measuring 0° phase angle bidirectional surface reflectance band ratios using four different wavelengths in the SWIR (shortwave infrared) spectral region between 1 and 2 µm.

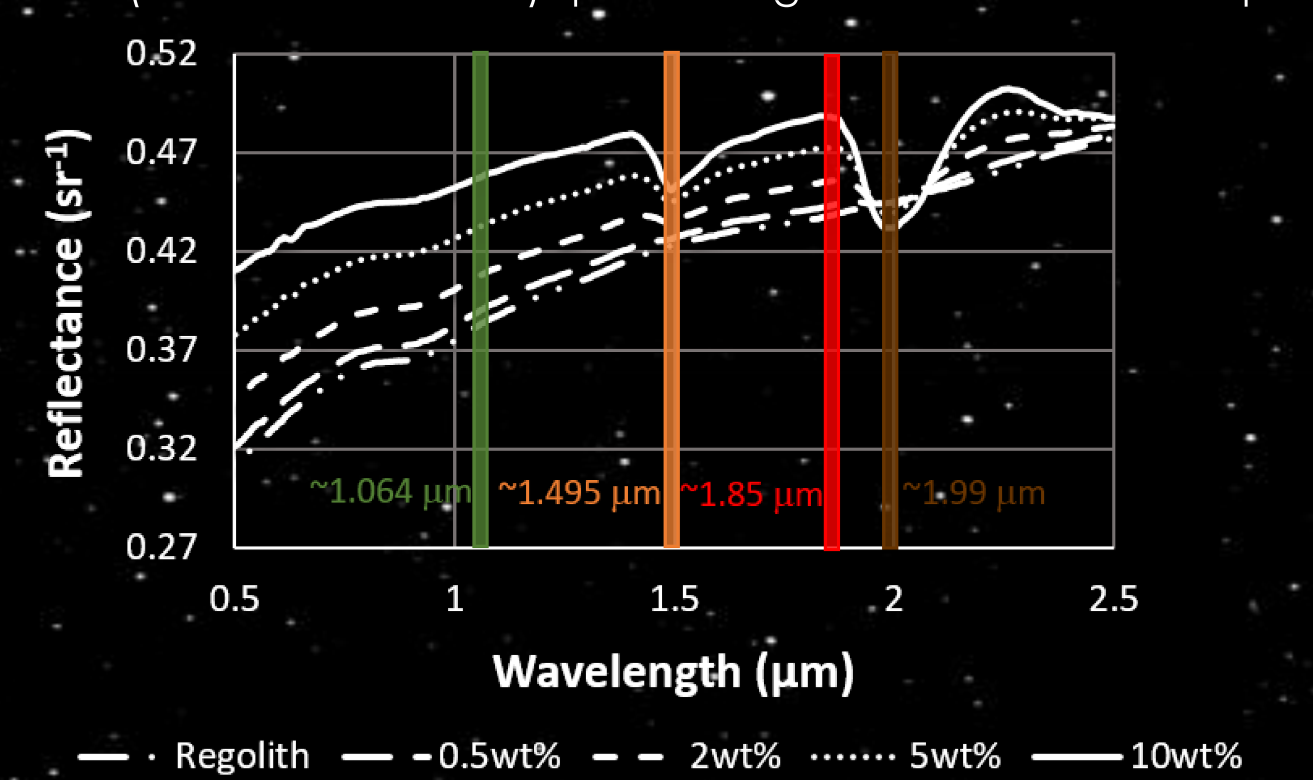

wt%: H_2O ice weight percent. Spectra calculated using Hapke theory [7], with water ice optical constants from [8] and a reflectance spectrum of Apollo 14 lunar highlands sample 14259-85.

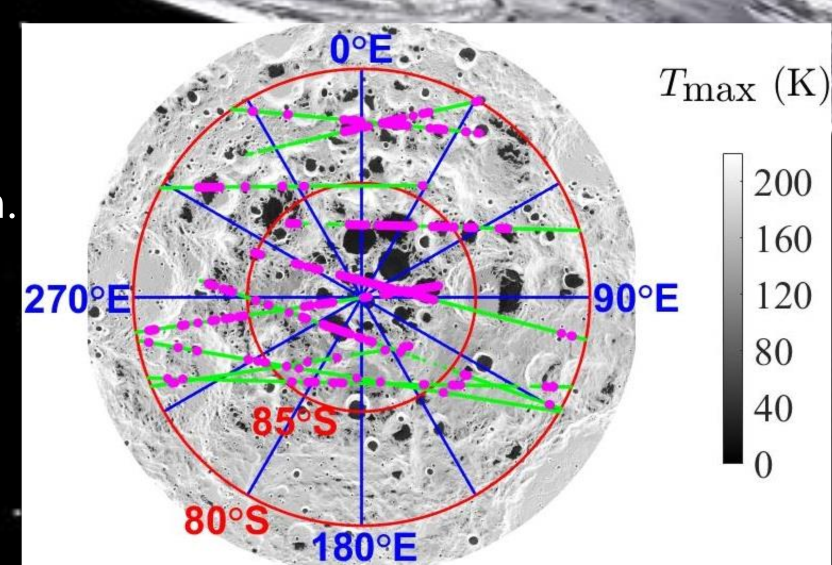

LF spacecraft Science data paths on the lunar South Pole. The gray scale shows the maximum temperature; the green and pink segments are the Science paths with the pink dots indicating the PSRs.

- The lasers fire sequentially for ≥ 6 ms , followed by a pause of ≥ 6 ms with all lasers off.
- When all lasers are off, background is measured and subtracted from the measured signals.
- In order to increase the SNR (Signal-to-Noise Ratio), measurements are averaged for each of the spectral band over the lunar ground-track corresponding to the desired mapping resolution.
- Continuum/absorption reflectance band ratios are then analyzed to quantify the weight percent of water ice (wt%) in the illuminated FOV (Field Of View).

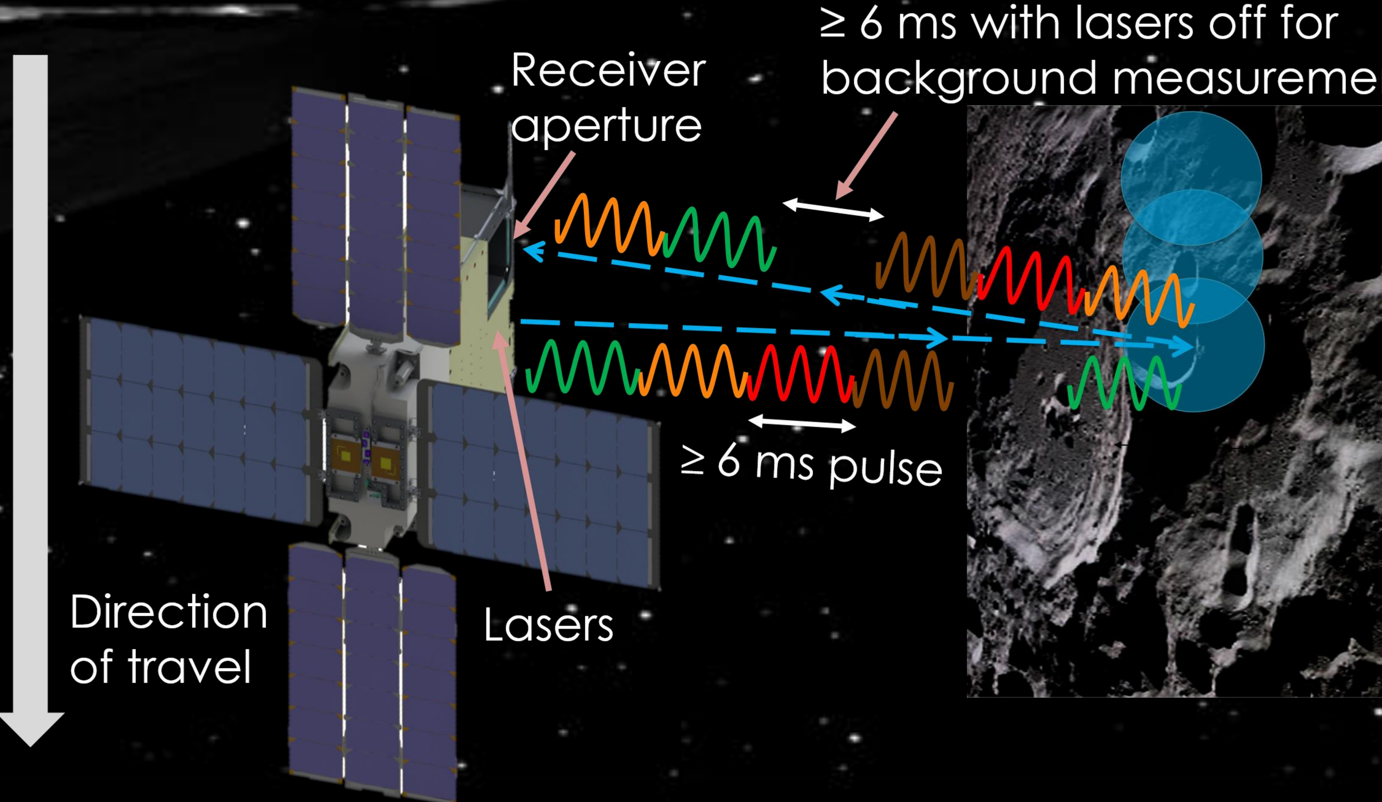

LF multi-band SWIR laser reflectometer

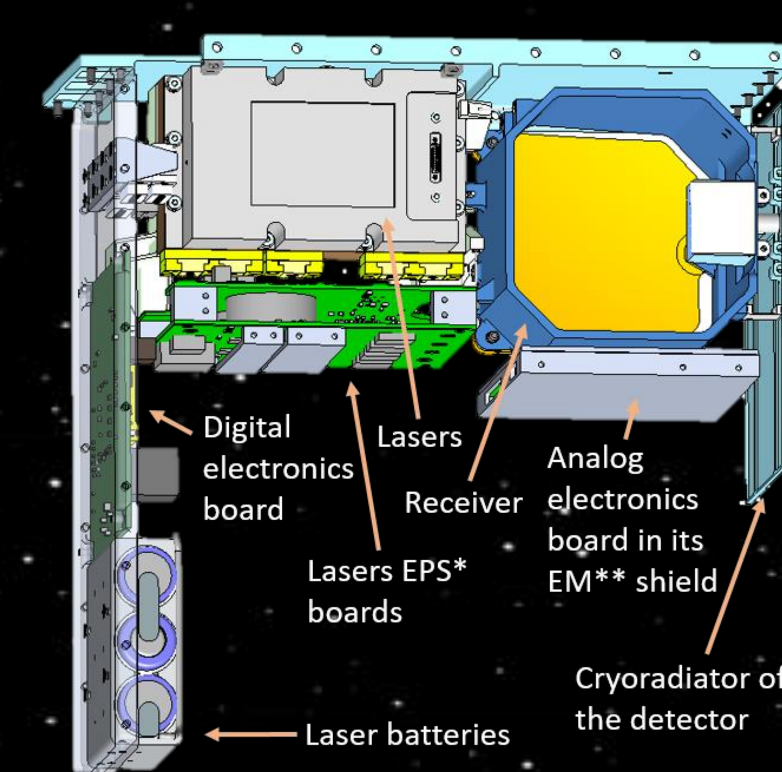

EPS*: Electrical Power System
EM**: ElectroMagnetic

- Optical receiver: 70×70-mm off-axis Al paraboloidal mirror; 70 mm focal length; single pixel 2 mm diameter InGaAs detector cooled at -65°C (1 nA dark current); 20.2 mrad uniform FOV; optimized for stray solar light rejection from outside the FOV.
- Detector reading electronics (analog board): 0-10 nA current range; 100 kHz sampling rate; 0.5 pA/Hz$^{1/2}$ RMS (Root Mean Square) Nyquist noise spectral density; 236 Hz 3dB-bandwidth.
- Diode lasers: 15-55 W optical power; wavelengths: ~1.495 & ~1.99 µm (H_2O ice absorption peaks) and ~1.064 & ~1.850 µm (nearby continuum); > 99.6% emitted energy encircled within 20.2 mrad.

System modeling

We have modeled Gaussian and systematic uncertainty sources as a function of the spacecraft position for each of the wavelength. From this, we evaluate the fraction of covered area for which the SNRs are high enough to discriminate between dry regolith and a given water ice content as a function of the confidence level. Below is the estimated error tree corresponding to a mapping resolution of 10 km (i.e. after averaging) and 6 ms pulses, using the two shortest wavelengths. TBD (To Be Determined) values have been set to zero.

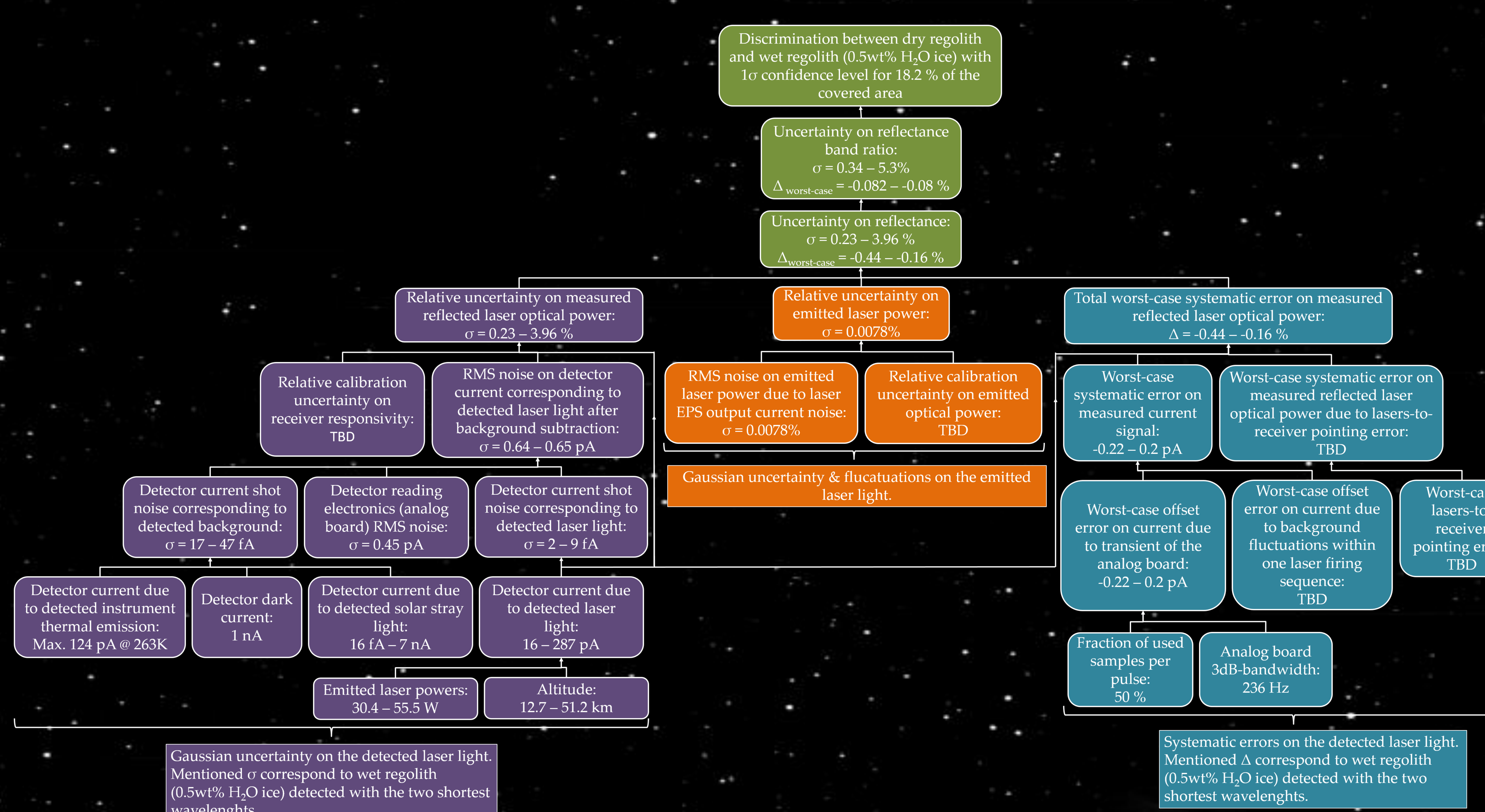

Results and Discussion

Mapping resolution: 10 km & Pulse width: 6 ms

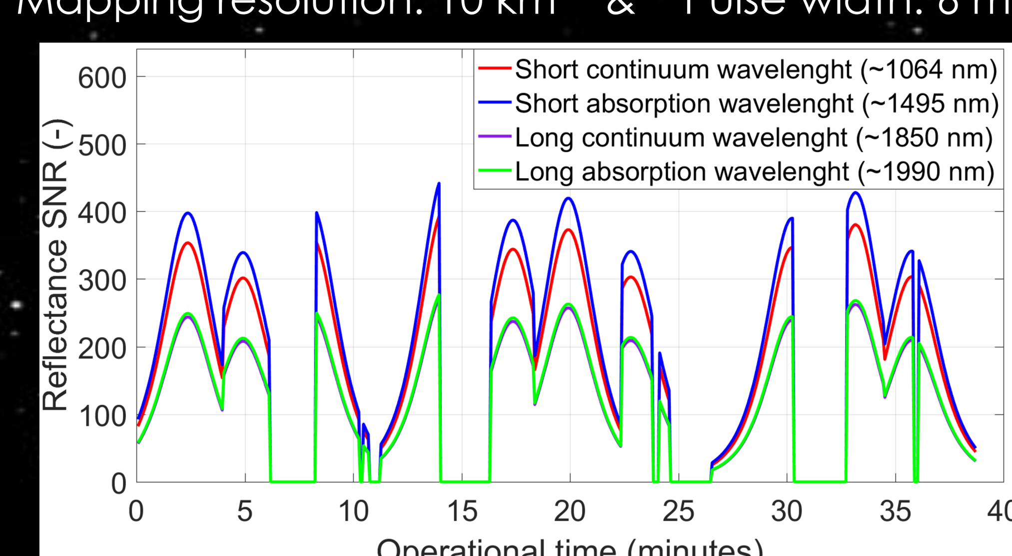

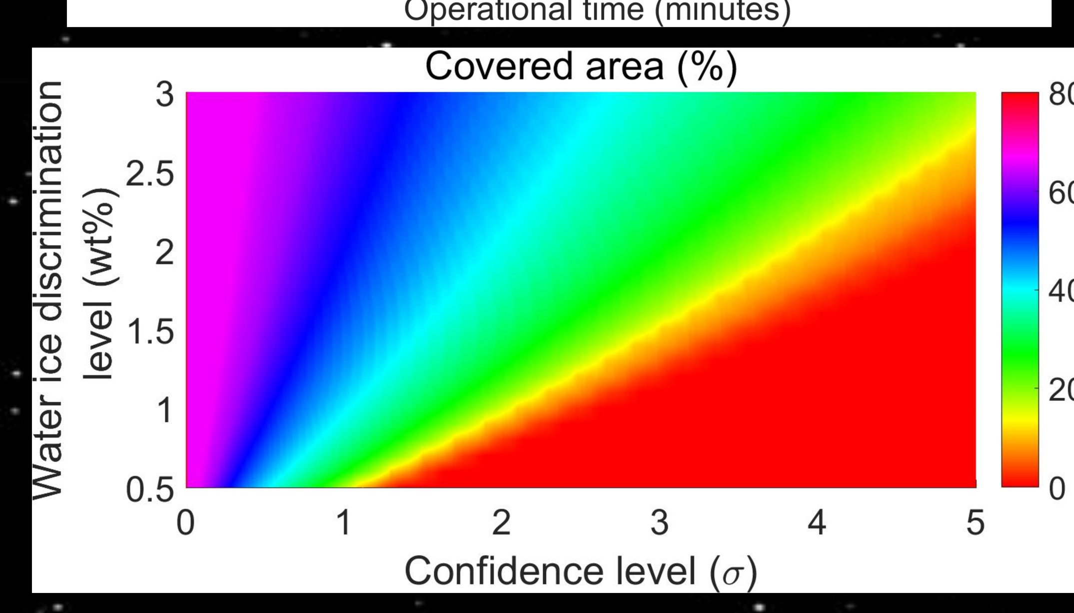

Conclusion:

- The detector reading electronics (analog board) constitutes the major source of noise. Noise performance is mainly driven by the challenging mass and volume (2U) constraints of the instrument.
- Thermal constraints, driven by mass and volume constraints, limit the laser power available, and thus the instrument SNR.
- Trade off between mapping resolution and instrument SNR.

Next steps:

- Finalize the system engineering phase to optimize the instrument SNR (lasers' power monitoring and pulse width VS background fluctuations & analog board bandwidth).
- Estimate TBD values in the error tree (achievable instrument calibration accuracy, background fluctuations impact, lasers-to-receiver pointing error) and finalize the calculations of the instrument performance.

[1] Paige, D. A., et al. (2010) Science, 330, 479-482. [2] Mitrofanov, I. G., et al. (2010) Science, 330, 483-486. [3] Gladstone, G. R., et al. (2012) JGR, 117, E00H04. [4] Zuber, M. T., et al. (2012) Nature, 486, 378-381. [5] Hayne, P. O., et al. (2015) Icarus, 255, 58-59. [6] McCord, T. B., et al. (2011) JGR, 116. [7] Hapke, B. (1981) JGR, 86(B4), 3039-3054. [8] Warren, S. G., & Brandt, R. E. (2008) JGR, 113(D14).